

Electron Attachment to the Lowest Unoccupied Orbitals in Linear and Branched Permethylated Polysilanes and Hexamethyldigermane and -distannane

Alberto Modelli*

Dipartimento di Chimica "G. Ciamician", Università di Bologna, via Selmi 2,
40126 Bologna, Italy

Derek Jones and Laura Favaretto

Istituto dei Composti del Carbonio Contenenti Eteroatomi e Loro Applicazioni, CNR,
via Gobetti 101, 40129 Bologna, Italy

Giuseppe Distefano

Dipartimento di Chimica, Università di Ferrara, via Borsari 46, 44100 Ferrara, Italy

Received August 7, 1995[Ⓢ]

The peculiar properties of polysilanes have stimulated many studies of their electronic structure. While the nature and ordering of the filled MOs have been studied in some detail, the theoretical predictions for the empty counterparts have never been tested experimentally. Here the electron transmission spectra of $\text{Me}(\text{SiMe}_2)_n\text{Me}$ (with $\text{Me} = \text{CH}_3$ and $n = 1-4$), $\text{MeSi}(\text{SiMe}_3)_3$, $\text{Si}(\text{SiMe}_3)_4$, Ge_2Me_6 , and Sn_2Me_6 are presented and the energies of the observed resonances allow assignment of the lowest unoccupied levels. With the change from monomers to dimers, the presence of a heteroatom-heteroatom bond causes a large electron affinity increase; the LUMO is ascribed to a σ^* MO essentially heteroatom in character, whereas the lowest $\sigma^*_{\text{C-heteroatom}}$ MOs lie at about 1.5 eV higher energy. The spectra of the linear trimer and tetramer of silicon show that the energy separation between the lowest-lying empty orbitals is even larger than that observed in their filled counterparts. The lowest-lying empty MOs are thus well delocalized on the silicon skeleton but not on the substituents. The resonance energies are also compared with the unoccupied orbital energies calculated by means of *ab initio* 3-21G* and MNDO methods. The results presented here do not support the previously proposed π^* model based upon *ab initio* calculations.

Introduction

Electron transmission spectroscopy (ETS)¹ is one of the most suitable means for studying the virtual orbital structure of gas-phase molecular systems. This technique takes advantage of the sharp variations in the electron-molecule scattering cross section associated with temporary electron capture into vacant orbitals. The energies (attachment energies, AEs) at which these resonance processes occur are the negative of electron affinities. Temporary anion states associated with empty σ^* orbitals generally lie at higher energy and have a shorter lifetime with respect to those associated with π^* orbitals, thus giving rise to broader shape resonances in electron transmission spectroscopy. In the ET spectrum of *n*-pentane,² for instance, no σ^* resonances have been observed. However, our systematic ET investigation on hydrocarbons containing group 14,^{3,4} group 15,⁵ group 16,⁶⁻¹¹ and group 17¹²⁻¹⁹ het-

eroatoms showed that the presence of a third-row element gives rise to low-energy σ^* resonances, not displayed in the spectra of the second-row analogues, and that the electron affinity further increases on going down the groups. According to MS-X α calculations^{5,8,17-19} the lowest σ^* orbital is mainly localized at the third-row (or heavier) element and possesses a large d character. The next step in our investigation on the electron-acceptor properties of heterosubstituted satu-

(7) Modelli, A.; Jones, D.; Colonna, F. P.; Distefano, G. *Chem. Phys.* **1983**, *77*, 153.

(8) Guerra, M.; Distefano, G.; Jones, D.; Colonna, F. P.; Modelli, A. *Chem. Phys.* **1984**, *91*, 383.

(9) Modelli, A.; Guerra, M.; Jones, D.; Distefano, G.; Irgolic, K. J.; French, V.; Pappalardo, G. *Chem. Phys.* **1984**, *88*, 455.

(10) Modelli, A.; Distefano, G.; Guerra, M.; Jones, D.; Rossini, S. *Chem. Phys. Lett.* **1986**, *132*, 448.

(11) Modelli, A.; Jones, D.; Distefano, G.; Tronc, M. *Chem. Phys. Lett.* **1991**, *181*, 361.

(12) Burrow, P. D.; Modelli, A.; Chiu, N. S.; Jordan, K. D. *Chem. Phys. Lett.* **1981**, *82*, 270.

(13) Burrow, P. D.; Modelli, A.; Chiu, N. S.; Jordan, K. D. *J. Chem. Phys.* **1982**, *77*, 2699.

(14) Modelli, A.; Burrow, P. D. *J. Electron Spectrosc.* **1983**, *32*, 263.

(15) Burrow, P. D.; Modelli, A.; Jordan, K. D. *Chem. Phys. Lett.* **1986**, *132*, 441.

(16) Modelli, A.; Foffani, A.; Scagnolari, F.; Jones, D. *Chem. Phys. Lett.* **1989**, *163*, 269.

(17) Modelli, A.; Scagnolari, F.; Distefano, G.; Guerra, M.; Jones, D. *Chem. Phys.* **1990**, *145*, 89.

(18) Guerra, M.; Jones, D.; Distefano, G.; Scagnolari, F.; Modelli, A. *J. Chem. Phys.* **1991**, *94*, 484.

(19) Modelli, A.; Scagnolari, F.; Distefano, G.; Jones, D.; Guerra, M. *J. Chem. Phys.* **1992**, *96*, 2061.

* Abstract published in *Advance ACS Abstracts*, November 15, 1995.

(1) Sanche, L.; Schulz, G. J. *J. Phys. Rev.* **1972**, *A5*, 1672.

(2) Schafer, O.; Allan, M.; Szeimies, G.; Sanktjohanser, M. *J. Am. Chem. Soc.* **1992**, *114*, 8180.

(3) Modelli, A.; Jones, D.; Distefano, G. *Chem. Phys. Lett.* **1982**, *86*, 434.

(4) Modelli, A.; Distefano, G.; Jones, D.; Seconi, G. *J. Electron Spectrosc. Relat. Phenom.* **1983**, *31*, 63.

(5) Modelli, A.; Distefano, G.; Guerra, M.; Jones, D.; Rossini, S. *Chem. Phys.* **1988**, *125*, 389.

(6) Modelli, A.; Distefano, G.; Jones, D. *Chem. Phys.* **1982**, *73*, 395.

rated hydrocarbons was to measure the evolution of the electron affinity values in derivatives containing an S–S or an Se–Se bond.¹¹ The ET spectra showed an additional resonance at considerably lower energy with respect to the corresponding monochalcogenides, indicating that the lowest singly occupied molecular orbital (SOMO) in the anions or, within the validity of Koopmans' theorem,²⁰ the lowest unoccupied molecular orbital (LUMO) in the neutral molecules is mainly localized at the chalcogen–chalcogen bond. We extend here the gas-phase ETS analysis to permethylated group 14 saturated compounds containing heteroatom–heteroatom bonds, in particular to linear and branched polysilanes and to hexamethyldigermene and -distannane.

Over the last 10 years, polysilanes have attracted large attention owing to their interesting mechanical, physical, and electronic properties. Polysilanes absorb strongly in the UV region at sizeably lower energy than the corresponding alkanes, their behavior in this regard resembling more that of unsaturated hydrocarbons. The reduced spectral band gap confers conducting properties to doped polymers, explained by extensive $\sigma_{\text{Si-Si}}$ delocalization. Irradiation of linear silicon catenates causes bond scission and formation of silyl radicals. This photolability finds applications in the initiation of polymerization reactions. These and other interesting applications of polysilanes, due to their thermal and oxidative stability and their capacity to form thin films, are described in ref 21. The peculiar and important properties of polysilanes stimulated theoretical and experimental studies aimed at the characterization of their electronic structure. Several photoelectron spectroscopy measurements^{22–25} provided the ionization energies from the valence filled orbitals of polysilanes and of permethylated derivatives. These data demonstrated that the outermost filled MOs are strongly delocalized and that they possess mainly $\sigma_{\text{Si-Si}}$ character. *Ab initio* calculations^{26,27} demonstrated to be suitable for reproducing the experimental filled energy levels confirmed the $\sigma_{\text{Si-Si}}$ nature and the large delocalization of the outermost MOs and the lower energy of the $\sigma_{\text{Si-H}}$ MOs. 3-21G, 3-21G*, and more extended basis set (even including CI) *ab initio* calculations on neutral linear²⁷ and cyclic^{28,29} polysilanes also provided a picture of the LUMOs as π -shaped orbitals with large contributions from the H atoms (or the C atoms in cyclic permethylated derivatives), bonding between the Si atoms and antibonding between the Si and H (or C) atoms. Miller and Michl³⁰ described the lowest empty orbitals in linear polysilanes as Si–Si antibonding; however, in agreement with the π type empty orbital model cited above, they confirmed the strong $3p_y$ (and

3s) character of the lowest-lying empty orbitals, as opposed to the essentially $3p_z$ character of the outermost filled orbitals (where z is used to label the long axis of the Si chain and y for the short in-plane axis). Grev and Schaefer²⁸ pointed out that single-configuration SCF calculations, even extending the basis set and including more and more diffuse functions, are not expected to be reliable in describing the empty level structure and that the validity of the π^* model rests in its ability to account for experimental data. The energies calculated^{27,28} for the various empty orbitals in the linear polysilanes $\text{H}(\text{SiH}_2)_n\text{H}$, however, could not be compared with experiment, owing to the absence of gas-phase electron affinity data. To date, the only experimental data²⁹ reported in the literature are the attachment energies to the LUMO in the five- and six-membered permethylated rings, both slightly below 2 eV. The results of a ²⁹Si ENDOR study³¹ were found to be hardly consistent with the *ab initio* π -type empty orbital model, suggesting a $\sigma^*_{\text{Si-Si}}$ or Si 3d character of the SOMO in cyclopolysilane anion radicals, and ESR studies³² on analogous molecular systems lead to a representation of the SOMO as a linear combination of $\sigma^*_{\text{Si-C}}$ and $\sigma^*_{\text{Si-Si}}$ orbitals. According to recent *ab initio* studies at the MP4SDTQ level on the disilane³³ and digermene³⁴ radical anions, the SOMO is a heteroatom–heteroatom σ^* antibonding orbital with a large heteroatom s diffuse orbital contribution, while the participation of Si 3d or Ge 4d orbitals is found to be negligibly small. We therefore have an uncertain picture of the low-energy unoccupied orbitals in such compounds. The most correct theoretical approach for estimating the impact energies at which shape resonance processes are observed in ETS is, in principle, the calculation of the total electron scattering cross section with the use of continuum functions, although an accurate description of the electron–molecule interactions involves difficulties.³⁵ Alternatively, bound-state calculations can be used but in conjunction with stabilization methods.³⁶ The present paper gives for the first time the experimentally measured energies of electron attachment to the low-energy empty orbitals and their evolution with increasing numbers of Si atoms in linear and branched polysilanes. These data can be used as a reference for the suitability of theoretical methods in reproducing the empty level structure in these compounds, just as the photoelectron data did for the filled counterpart. The molecular systems analyzed are listed in Chart 1.

Experimental Details and Calculations

Our ETS apparatus³ is in the format devised by Sanche and Schulz.¹ An electron beam with a typical resolution of 40 meV fwhm is passed through a collision cell containing the vapor of the sample of interest. At energies at which electron capture into a normally unoccupied orbital occurs, there is a change in the scattering cross section and, hence, in the transmitted current. The derivative with respect to energy of the transmitted current, as a function of the incident electron energy, is recorded. The present spectra have been obtained by using

- (20) Koopmans, T. A. *Physica* **1933**, *1*, 104.
 (21) Miller, R. D. *Angew. Chem., Int. Ed. Engl.* **1989**, *28*, 1733.
 (22) Bock, H.; Ensslin, W.; Feher, F.; Freund, R. *J. Am. Chem. Soc.* **1976**, *98*, 668.
 (23) Ensslin, W.; Bergmann, H.; Elbel, S. *J. Chem. Soc., Faraday Trans. 2* **1975**, *71*, 913.
 (24) Pitt, C. G.; Carey, R. N.; Toren, E. C. *J. Am. Chem. Soc.* **1972**, *94*, 3806.
 (25) Bock, H.; Ensslin, W. *Angew. Chem., Int. Ed. Engl.* **1971**, *10*, 404.
 (26) Ortiz, J. V.; Mintmire, J. W. *J. Am. Chem. Soc.* **1988**, *110*, 4522.
 (27) Nelson, J. T.; Pietro, W. J. *J. Phys. Chem.* **1988**, *92*, 1365.
 (28) Grev, R. S.; Schaefer, H. F., III. *J. Am. Chem. Soc.* **1987**, *109*, 6569.
 (29) Tossell, J. A.; Winkler, D. C.; Moore, J. H. *Chem. Phys.* **1994**, *185*, 297.
 (30) Miller, R. D.; Michl, J. *J. Am. Chem. Soc.* **1989**, *89*, 1359.

- (31) Kirste, B.; West, R.; Kurreck, H. *J. Am. Chem. Soc.* **1985**, *107*, 3013.
 (32) Wadsworth, C. L.; West, R. *Organometallics* **1985**, *4*, 1664.
 (33) Tada, T. *Chem. Phys. Lett.* **1990**, *173*, 15.
 (34) Tada, T.; Yoshimura, R. *J. Phys. Chem.* **1993**, *97*, 1019.
 (35) Lane, N. F. *Rev. Mod. Phys.* **1980**, *52*, 29.
 (36) Hazi, A. U.; Taylor, H. S. *Phys. Rev. A* **1970**, *1*, 1109.

Chart 1

1	Si(CH ₃) ₄	tetramethylsilane
2	Si ₂ (CH ₃) ₆	hexamethyldisilane
3	Si ₃ (CH ₃) ₈	octamethyltrisilane
4	Si ₄ (CH ₃) ₁₀	decamethyltetrasilane
5	CH ₃ Si[Si(CH ₃) ₃] ₃	tris(trimethylsilyl)methylsilane
6	Si[Si(CH ₃) ₃] ₄	tetrakis(trimethylsilyl)silane
7	(CH ₃) ₃ SiCH ₂ Si(CH ₃) ₃	bis(trimethylsilyl)methane
8	(CH ₃) ₃ SiOSi(CH ₃) ₃	bis(trimethylsilyl)oxide
9	(CH ₃) ₃ SiSSi(CH ₃) ₃	bis(trimethylsilyl)sulfide
10	Ge(CH ₃) ₄	tetramethylgermane
11	Sn(CH ₃) ₄	tetramethyltin
12	Ge ₂ (CH ₃) ₆	hexamethylgermane
13	Sn ₂ (CH ₃) ₆	hexamethyldistannane

the apparatus in the "high rejection" mode, unless otherwise specified, which yields a signal related to the nearly total cross section.³⁷ The attachment energies given correspond to the vertical midpoints between minima and maxima in the differentiated signal. The energy scales have been calibrated with reference to the (1s¹2s²) anion state in He. The estimated accuracy is ±0.05 or ±0.1 eV, depending on the number of decimal digits reported.

The linear Si₃(CH₃)₈^{38,39} (3) and Si₄(CH₃)₁₀³⁹ (4) and the branched CH₃Si[Si(CH₃)₃]₃⁴⁰ (5) and Si[Si(CH₃)₃]₄⁴¹ (6) were prepared according to previously described methods. The remaining compounds are commercially available.

Ab initio 3-21 G* and MNDO calculations were performed for tetramethylsilane (*T_d* point group) and for the linear permethylated di (*D_{3d}*), tri- (*C_{2v}*), and tetrasilane (*C_{2h}*), allowing relaxation of all the internal parameters. As reported below, the *ab initio* results are in better agreement with available geometrical data but are unable to reproduce the main features of the ET spectra. For this reason, computations on the tris(trimethylsilyl)- and tetrakis(trimethylsilyl)-branched derivatives (*C_{3v}* and *T_d*, respectively) were carried out at the MNDO level only.

Results and Discussion

Computational Results. The above mentioned π* model in linear polysilanes is based on the results of *ab initio* 3-21G*, or more sophisticated, calculations. We apply the 3-21G* calculations to the permethylated linear polysilanes in order to verify whether substitution of the hydrogen atoms with methyl groups should lead to significant changes in the energy and nature of the lowest unoccupied orbitals. Our aim is to examine the validity of the π* model by comparison with the experimentally determined energies and assignments. We also compare the experimental data with the results of simple MNDO semiempirical calculations, which include correlation and relaxation indirectly, *via* parametrization.⁴⁴ Table 1 compares the Si–Si and Si–C bond distances computed for linear permethylated silanes with available experimental data. The MNDO values are nearly constant along the monomer–tetramer series and shorter than the experimental ones. The bond lengths calculated at the *ab initio* level are in much better agreement with experiment. The energy ordering and symmetries of the outermost filled MOs in linear

Table 1. Experimental and Calculated Si–Si and Si–C Bond Lengths (Å)

	exptl	<i>ab initio</i> 3-21 G*	MNDO
Si–Si	2.325 ^a	2.35–2.36 ^b	2.21
Si–C	1.875 ^c –1.887 ^a	1.89–1.91 ^b	1.82

^a Electron diffraction bond lengths in Si₃(CH₃)₈ from ref 42.
^b Range of values computed in the monomer–tetramer series.
^c Electron diffraction bond length in Si(CH₃)₄ from ref 43.

Table 2. *Ab Initio* 3-21G* and MNDO Energies (eV) of the Frontier MOs for the Linear Permethylated Oligosilanes Me(SiMe₂)_nMe with Me = CH₃ and n = 1–4 and for the Branched CH₃Si(SiMe₃)₃ (5) and Si(SiMe₃)₄ (6)

molecule	orbital	3-21G*		MNDO	
		energy	sym	energy	sym
1 (<i>T_d</i>)	2nd LUMO	7.11	t ₂	3.70	a ₁
	LUMO	6.63	a ₁	2.25	t ₂
	HOMO	–11.14	t ₂	–11.34	t ₂
2 (<i>D_{3d}</i>)	3rd LUMO	6.67	a _{2u}	1.97	e _g
	2nd LUMO	6.23	a _{1g}	1.85	e _u
	LUMO	5.12	e _u	0.16	a _{2u}
	HOMO	–9.42	a _{1g}	–9.72	a _{1g}
	2nd HOMO	–11.30	e _g	–11.35	e _g
3 (<i>C_{2v}</i>)	3rd LUMO	5.74	b ₂	1.65	b ₁
	2nd LUMO	4.44	b ₁	0.33	a ₁
	LUMO	4.33	a ₁	–0.18	b ₂
	HOMO	–8.89	b ₂	–9.32	b ₂
	2nd HOMO	–10.00	a ₁	–10.28	a ₁
4 (<i>C_{2h}</i>)	3rd HOMO	–11.25	b ₁	–11.36	b ₁
	5th LUMO	5.44	b _u	1.71	b _g
	4th LUMO	5.41	b _g	1.65	a _u
	3rd LUMO	4.91	a _g	0.24	b _u
	2nd LUMO	4.39	a _u	0.10	a _g
5 (<i>C_{3v}</i>)	LUMO	3.60	b _u	–0.42	b _u
	HOMO	–9.44	a _g	–9.08	a _g
	2nd HOMO	–9.89	b _u	–9.92	b _u
	3rd HOMO	–9.98	a _g	–10.38	a _g
	4th HOMO	–11.26	b _g	–11.43	b _g
	3rd LUMO			2.15	e
	2nd LUMO			0.90	a ₁
6 (<i>T_d</i>)	LUMO			–0.07	e
	HOMO			–9.73	e
	2nd HOMO			–10.86	a ₁
	3rd HOMO			–11.37	a ₂
	5th LUMO			2.71	a ₁
	2nd LUMO			2.19	e
6 (<i>T_d</i>)	LUMO			0.03	t ₂
	HOMO			–10.24	t ₂
	2nd HOMO			–11.34	t ₁
	5th HOMO			–11.77	a ₁

permethylated silanes provided by the present 3-21G* calculations parallel those obtained for the corresponding unsubstituted silanes by previous *ab initio* calculations.^{26–28} Namely, the oligomethylsilanes possess high-lying σ MOs delocalized mainly along the silicon skeleton. These orbitals lie well above those of prevalent substituent character. Orbital energies and symmetries are listed in Table 2, together with the MNDO results. The results provided by the two methods for the filled orbitals are equivalent. Comparison of the present 3-21G* calculations with previous *ab initio* results^{27,28} on unsubstituted linear silanes shows that also for the lowest lying virtual orbitals the calculated energy ordering and nature (once replacement of methyl groups for the hydrogen atoms is taken into account) are not affected by permethylation. The unoccupied orbitals are mainly Si–Si bonding and Si–C antibonding, in line with the above mentioned π* model (see Figure 1). At variance with the results for the filled orbitals, the empty orbital structure predicted by the MNDO calculations is quite different from the *ab initio*

(37) Johnston, A. R.; Burrow, P. D. *J. Electron Spectrosc. Relat. Phenom.* **1982**, 25, 119.

(38) Kumada, M. *J. Org. Chem.* **1956**, 21, 1264.

(39) Kumada, M. *J. Organomet. Chem.* **1963**, 1, 153.

(40) Gilman, H.; Harrell, R. L. *J. Organomet. Chem.* **1966**, 5, 199.

(41) Gilman, H.; Smith, C. L. *J. Organomet. Chem.* **1967**, 8, 245.

(42) Almenningen, A.; Fjeldberg, T.; Hengge, E. *J. Molec. Struct.* **1984**, 112, 239.

(43) *CRC Handbook of Chemistry and Physics*, 73rd ed.; Lide, D. R., Ed.; CRC Press: Boca Raton, FL, 1992.

(44) Clark, T. In *A Handbook of Computational Chemistry*; J. Wiley: New York, 1985; Chapter 4.

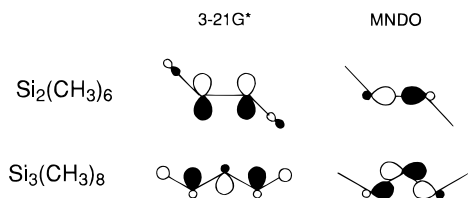


Figure 1. Schemes of the LUMOs in hexamethyldisilane (**2**) and octamethyltrisilane (**3**) as deduced from *ab initio* and MNDO calculations.

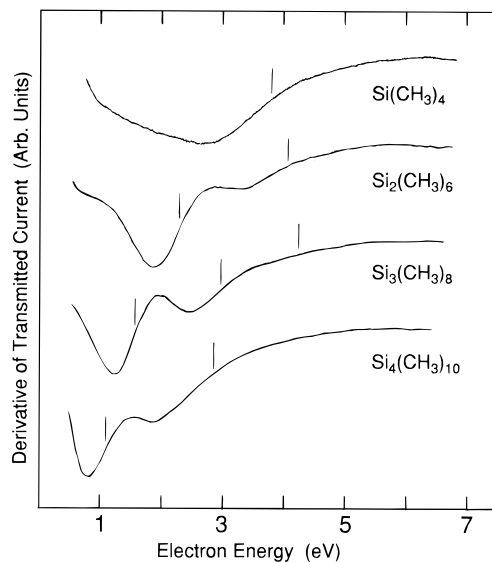


Figure 2. Derivative of the electron current transmitted through the gas-phase linear permethylated silanes $\text{Me}(\text{SiMe}_2)_n\text{Me}$ (**1–4**), as a function of the incident electron energy. Vertical lines locate the most probable AE values.

results (see Table 2). At the *ab initio* level, the low-lying virtual orbitals in linear permethylated polysilanes are delocalized over the silicon, carbon, and hydrogen atoms, whereas, according to the MNDO results, there are a number of singly degenerate low-lying empty orbitals, equal to the number of Si–Si bonds, which possess almost exclusively silicon character. The empty orbitals with sizable carbon and hydrogen contributions lie well above in energy. Figure 1 reveals another relevant difference between the MNDO and *ab initio* empty level pictures, which is concerned with the bonding properties of the LUMOs. In contrast with the *ab initio* π^* model, the MNDO calculations predict an antibonding character between Si atoms, as normally expected for σ^* orbitals. MNDO calculations have also been carried out for the branched derivatives $\text{CH}_3\text{Si}[\text{Si}(\text{CH}_3)_3]_3$ (**5**, C_{3v}) and $\text{Si}[\text{Si}(\text{CH}_3)_3]_4$ (**6**, T_d), and the results have been included in Table 2.

Silicon Derivatives. Figure 2 displays the ET spectra of tetramethylsilane and of the linear permethylated polysilanes up to $\text{Si}_4(\text{CH}_3)_{10}$. The vertical AEs measured in these compounds are reported in Figure 3 together with a diagram of the first ionization energies, taken from ref 25. The lowest-lying signal shown by the ET spectrum of tetramethylsilane (**1**) is a rather broad resonance centered at 3.8 eV. According to the *ab initio* results the LUMO possesses a_1 symmetry, whereas the MNDO calculations predict the LUMO to be triply degenerate. As previously⁴ deduced by comparison between the hyperconjugative energy perturbations brought about by the $-\text{Si}(\text{CH}_3)_3$ and $-\text{CH}_2\text{Si}(\text{CH}_3)_3$

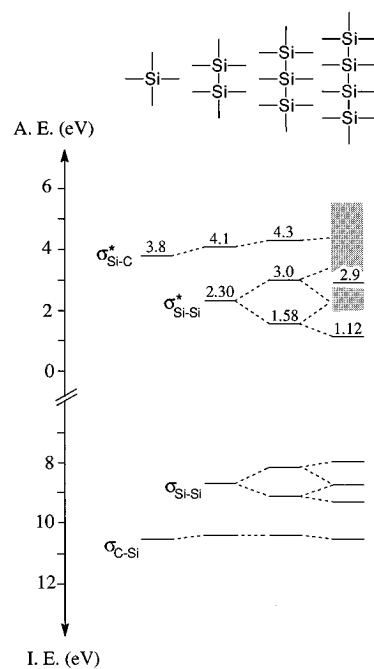


Figure 3. AE values and correlation diagram of the frontier orbitals in the gas-phase linear permethylated silanes $\text{Me}(\text{SiMe}_2)_n\text{Me}$ (**1–4**), as obtained by ETS and photoelectron spectroscopy, respectively. Ionization energies are taken from ref 25.

groups on adjacent π and π^* orbitals, the participation of the silicon atom should be larger in the σ^* LUMO than in the filled counterpart (HOMO), in line with the smaller electronegativity of the silicon atom with respect to the carbon atom. With the change from tetramethylsilane to hexamethyldisilane, the first anion state is largely stabilized. A similar electron affinity increase was observed on going from $\text{S}(\text{CH}_3)_2$ to $\text{CH}_3\text{S}-\text{SCH}_3$.¹¹ The first resonance (2.30 eV) displayed by the ET spectrum of $(\text{CH}_3)_3\text{Si}-\text{Si}(\text{CH}_3)_3$ (**2**) is well separated in energy from the higher-lying signals arising from $\sigma^*_{\text{Si}-\text{C}}$ MOs and is thus ascribed to an empty orbital mainly localized at the Si–Si bond, in agreement with the MNDO results. The energy location of the corresponding filled $\sigma_{\text{Si}-\text{Si}}$ orbital is symmetrical (see Figure 3), so that the presence of a Si–Si bond in a saturated hydrocarbon causes a corresponding increase in the electron-acceptor and the electron-donor properties at one and the same time. This suggests that the extent of interaction between the atomic orbitals of the Si and C atoms is larger than that between two Si atoms. In agreement, the strength of the Si–C bond is higher than that of the Si–Si bond.⁴³ In octamethyltrisilane (**3**), where two Si–Si bonds are present, an in-phase and an out-of-phase combination of the empty orbitals are expected. In fact, two resonances are observed (1.58 and 3.0 eV), whose splitting is exactly symmetrical with respect to the LUMO in $\text{Si}_2(\text{CH}_3)_6$. This retention of the baricenter, previously noted by Bock and Ensslin²⁵ in the corresponding filled orbitals, suggests that also the empty $\sigma^*_{\text{Si}-\text{Si}}$ orbitals, as predicted by the MNDO calculations, weakly mix with the $\sigma^*_{\text{Si}-\text{C}}$ orbitals. The photoabsorption spectrum of Si_3H_8 , near the edge of Si 2p ionization, does not provide information on the energy separation between the first two empty orbitals, which give rise to an unresolved broad (about 2 eV, fwhm) signal.⁴⁵ An interesting finding in the ET spectrum of $\text{Si}_3(\text{CH}_3)_8$ is that the energy separation (1.42

eV) between the two empty $\sigma^*_{\text{Si-Si}}$ orbitals is even larger than that (0.95 eV) measured in the filled counterparts. The smaller excitation energies in silicon catenates with respect to alkanes and the red shift observed in the absorption spectra as their chain length increases⁴⁶ are thus accounted for not only by decreasing ionization energies but also (and to a larger extent) by increasing electron affinities. The ET spectrum of the linear tetrasilicon derivative (**4**) displays a first resonance located at 1.12 eV and a very broad (3.7 eV fwhm) unresolved resonance at higher energy. This lack of resolution is not surprising, due to the increased number of empty orbitals and to the inverse dependence of anion state lifetime on energy. A linear combination bond orbitals (LCBO) approach⁴⁷ applied to the filled orbitals, taking the HOMO ionization energy measured in $\text{Si}_2(\text{CH}_3)_6$ as the Coulomb integral and half the difference between the first two MOs in $\text{Si}_3(\text{CH}_3)_8$ as the resonance integral, reproduces the first three ionization energy values of $\text{Si}_4(\text{CH}_3)_{10}$ to within ± 0.07 eV. An analogous approach applied to the empty orbitals also reproduces rather well the energy of electron attachment to the LUMO (calculated 1.29 eV, experimental 1.12 eV) and predicts the second and third resonances to lie at 2.30 and 3.31 eV. We therefore assign the broad signal centered at 2.9 eV (see Figure 3) to the unresolved contributions of the two highest $\sigma^*_{\text{Si-Si}}$ MOs and of higher-lying $\sigma^*_{\text{Si-C}}$ MOs. Extrapolation to a chain of infinite length using the LCBO method predicts an electron affinity (LUMO) for an ideal gas-phase polymer of -0.9 eV (i.e., $\text{AE} = 0.9$ eV) and an ionization energy (HOMO) of 7.7 eV. This would mean a reduction of 2.4 eV in the HOMO-LUMO energy gap on going from the dimer to the polymer (2.2 eV from the dimer to the octamer). These values are not inconsistent with the variation (1.64 eV) in λ_{max} observed in solution⁴⁶ on going from the dimer to the octamer. A comparison with the corresponding extrapolated electron affinity and ionization energy values of polythiophene⁴⁸ (+1.0 and 6.9 eV, respectively) indicates a lesser predisposition toward electrical conductivity for polymethylsilane. This is confirmed by the fact that conducting polysilanes have only been prepared using strong "doping" agents such as AsF_5 .²¹ The ET spectra indicate that in the $\text{Si}_2(\text{CH}_3)_6$ to $\text{Si}_4(\text{CH}_3)_{10}$ series there are a number of low-energy singly degenerate empty orbitals equal to the number of Si-Si bonds and that these orbitals arise from strong interactions between fragment orbitals largely localized at the Si atoms. These results seem therefore not to be in line with the π^* model proposed for the lower-lying empty orbitals by *ab initio* calculations. According to the *ab initio* calculations, the LUMO in $\text{Si}_2(\text{CH}_3)_6$ should be doubly degenerate (see Table 2), as well as in Si_2H_6 .^{27,28} In addition, the contributions from the silicon atoms should essentially arise from 3p atomic orbitals, not directed toward each other (see Figure 1 and ref 27). This would imply, even at a qualitative level, small overlap and extent of interaction. In fact, while the

energy separation (1.1 eV) calculated between the two outermost filled orbitals in $\text{Si}_3(\text{CH}_3)_8$ is in good agreement with experiment, the energy separation (0.1 eV) predicted between the two lowest empty orbitals is much smaller. This is at odds with the present ET data, according to which the lowest empty levels mirror the outermost filled levels but with even greater energy separation. Other *ab initio* results⁴⁹ predict for short linear oligosilanes low-energy σ^* empty orbitals interleaved and close in energy with π^* empty orbitals (that is, localized on the Si-H bonds and antisymmetric with respect to the plane containing the Si skeleton). The present ETS data show that the corresponding $\pi^*_{\text{Si-C}}$ resonances are located well above in energy than the lowest σ^* resonances, but of course the permethylated oligosilanes do not contain Si-H bonds. A representation of the lower-lying empty level structure of polysilanes in terms of strongly delocalized $\sigma^*_{\text{Si-Si}}$ orbitals, as given by the MNDO method and by an (SK)LCAO computational approach,⁵⁰ is more consistent with the ETS data. Also the UHF calculations by Tada³³ mentioned in the Introduction describe the SOMO in the disilane radical anion as a Si-Si antibonding σ^* orbital. The present MNDO calculations reproduce quite accurately the ionization energies from the filled $\sigma_{\text{Si-Si}}$ and $\sigma_{\text{Si-C}}$ orbitals (except for a constant shift of about 1 eV), as well as the constancy of the mean $\sigma_{\text{Si-Si}}$ ionization energies along the series. For the empty levels, agreement with experiment is less satisfactory, mainly because calculations underestimate the energy separations among the $\sigma^*_{\text{Si-Si}}$ orbitals in the trimer and the tetramer. However, in agreement with the ET spectra, the MNDO results predict empty levels specular with respect to the filled counterparts, with low-lying singly degenerate $\sigma^*_{\text{Si-Si}}$ orbitals followed by $\sigma^*_{\text{Si-C}}$ orbitals at higher energy. As mentioned in the Introduction, the small hyperfine anisotropy for ^{29}Si shown by ENDOR results on radical anions³¹ was found consistent with Si-Si σ^* or 3d spin population but not with π^* delocalization, although it has been suggested²⁹ that, due to the large diffuseness in space of the LUMO, this finding could also be consistent with the π^* model. Further experimental support for the Si-Si antibonding nature of the LUMO in linear polysilanes (as opposed to the bonding character between Si atoms predicted by the π -type model) comes from the chain scission observed in cyclic voltammetry upon electron addition.⁵¹

Substitution of a methyl group by a $-\text{Si}(\text{CH}_3)_3$ group at the central Si atom of $\text{Si}_3(\text{CH}_3)_8$ (**3**) shows the effect of chain branching. The upper curve in Figure 4 is the ET spectrum of $\text{CH}_3\text{Si}[\text{Si}(\text{CH}_3)_3]_3$ (**5**). The first resonance lies at 1.49 eV, that is, at 0.35 eV higher energy with respect to the linear $\text{Si}_4(\text{CH}_3)_{10}$ isomer. It is to be noted, however, that the branched isomer possesses higher symmetry (C_{3v}) and that, as predicted by the present MNDO calculations, the LUMO is doubly degenerate. The second resonance in the spectrum is assigned to the $\sigma^*_{\text{Si-Si}}$ orbital of a_1 symmetry. Replacement of the last methyl group at the central Si atom leads to tetrakis(trimethylsilyl)silane $\text{Si}[\text{Si}(\text{CH}_3)_3]_4$ (**6**). The first resonance (1.21 eV) still lies at slightly higher energy than in the linear $\text{Si}_4(\text{CH}_3)_{10}$, but in this case

(45) Sutherland, D. G. J.; Bancroft, G. M.; Bozek, J. D.; Tan, K. H. *Chem. Phys. Lett.* **1992**, *199*, 341.

(46) Pitt, C. G.; Bursley, M. M.; Rogerson, P. F. *J. Am. Chem. Soc.* **1970**, *92*, 519.

(47) Hall, G. G. *Proc. R. Soc. London, Ser. A* **1951**, *205*, 541. Heilbronner, E.; Bock, H. *The HMO Model and Its Application*; Wiley: Chichester, England, 1976; Vol. 12.

(48) Jones, D.; Guerra, M.; Favaretto, L.; Modelli, A.; Fabrizio, M.; Distefano, G. *J. Phys. Chem.* **1990**, *94*, 5761.

(49) Balaji, V.; Michl, J. *Polyhedron* **1991**, *10*, 1265.

(50) Takeda, K.; Teramae, H.; Matsumoto, N. *J. Am. Chem. Soc.* **1986**, *108*, 8186.

(51) Diaz, A.; Miller, R. D. *J. Electrochem. Soc.* **1985**, *132*, 834.

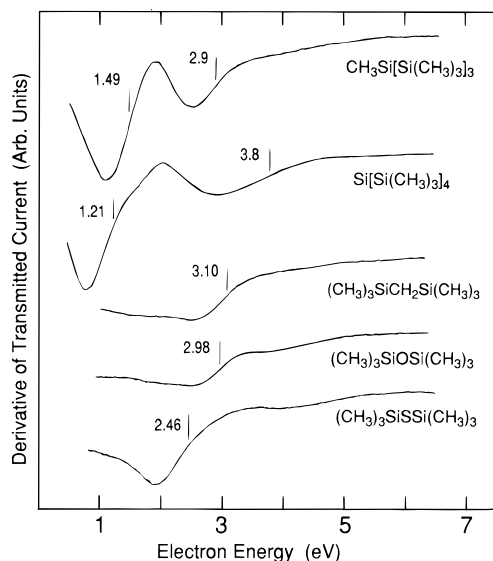


Figure 4. AE values and derivative of the electron current transmitted through gas-phase tris(trimethylsilyl)methylsilane (**5**), tetrakis(trimethylsilyl)silane (**6**), and the $\text{Me}_3\text{Si-X-SiMe}_3$ compounds (**7-9**), with $\text{X} = \text{CH}_2$, O , and S , as a function of the incident electron energy. Vertical lines locate the most probable AE values.

the LUMO, according to calculations, is triply degenerate. The calculations fail to reproduce the experimentally observed slight energy decrease of the LUMO, as well as the constancy of the HOMO energy,⁴⁶ on going from $\text{CH}_3\text{Si}[\text{Si}(\text{CH}_3)_3]_3$ (**5**) to $\text{Si}[\text{Si}(\text{CH}_3)_3]_4$ (**6**). However, in agreement with the ET spectra, they predict a large increase in the energy gap between the LUMO and the second empty MO. The second resonance in tetrakis(trimethylsilyl)silane (**6**), centered at 3.8 eV, should thus be associated with the unresolved contributions of the $\sigma^*_{\text{Si-Si}}$ (a_1) orbital and of $\sigma^*_{\text{Si-C}}$ MOs.

The bottom three ET spectra of Figure 4 show the effect of interruption of the Si-Si chain on the electron affinity. These molecules are obtained by replacement of the central $\text{Si}(\text{CH}_3)_2$ group in the linear trisilane $\text{Si}_3(\text{CH}_3)_8$ with a CH_2 group, O atom, or S atom, respectively. In bis(trimethylsilyl)methane (**7**) and in the oxygen derivative (**8**) the energy of the LUMO is lower than in tetramethylsilane but about 1.5 eV higher than in $\text{Si}_3(\text{CH}_3)_8$. In line with the presence of an additional third-row element, in $(\text{CH}_3)_3\text{Si-S-Si}(\text{CH}_3)_3$ (**9**) the ground anion state is somewhat (0.5 eV) more stable than in the CH_2 and O analogues **7** and **8** but still at about 0.9 eV higher energy with respect to the linear trisilane **3**.

Germanium and Tin Derivatives. Figure 5 displays the ET spectra of the permethylated monomers (**10** and **11**) and dimers (**12** and **13**) of germanium and tin. The AE values are given in the correlation diagram of Figure 6. Our calibration of the first resonance in tetramethylgermane is 0.3 eV lower than that previously reported in the literature.⁵² This discrepancy could, at least in part, stem from the broadness of the resonance and to the probable superposition of a low-intensity signal on the high-energy side, which does not

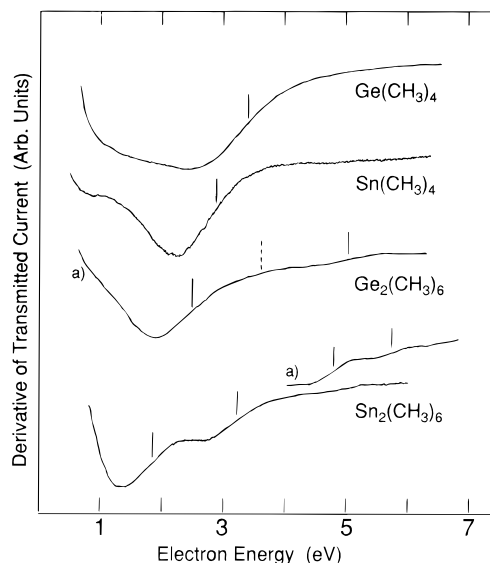


Figure 5. Derivative of the electron current transmitted through gas-phase tetramethylgermane (**10**) and -stannane (**11**) and through hexamethyldigermene (**12**) and -distannane (**13**), as a function of the incident electron energy. Vertical lines locate the most probable AE values. (a) Spectra recorded in the "low-rejection" mode.

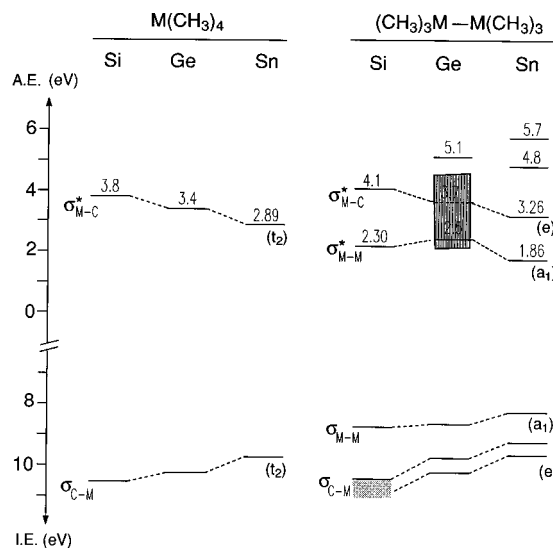


Figure 6. AE values and correlation diagrams of the frontier orbitals in gas-phase $\text{M}(\text{CH}_3)_4$ and $(\text{CH}_3)_3\text{M-M}(\text{CH}_3)_3$, with $\text{M} = \text{Si}$, Ge , and Sn , as obtained by ETS and photoelectron spectroscopy. Ionization energies taken from refs 53 (monomers) and 54 (dimers).

allow for accurate location of the resonance maximum in the derivative of transmitted current. As previously found in saturated hydrocarbons containing group 16¹¹ or group 17¹⁷ elements, the energy trends of the LUMOs and HOMOs on going down the group are symmetrical, the derivative of the heavier element being the best electron donor and electron acceptor at one and the same time. In particular, with the change from tetramethylsilane (**1**) to tetramethylstannane (**11**) the electron affinity increase (0.9 eV) and the ionization energy decrease are nearly of the same magnitude. The ET spectrum of hexamethyldistannane (**13**), as well as that of the silicon analogue, displays two well-resolved resonances at low energy, ascribed to electron capture into the $\sigma^*_{\text{Sn-Sn}}$ and to the lowest $\sigma^*_{\text{Sn-C}}$ orbitals, respectively. At variance, the "high-rejection" spectrum

(52) Giordan, J. C.; Moore, J. H. *J. Am. Chem. Soc.* **1983**, *105*, 6541.

(53) Evans, S.; Green, J. C.; Joachim, P. J.; Orchard, A. F.; Turner, D. W.; Maier, J. P. *J. Chem. Soc., Faraday Trans. 2* **1972**, *68*, 905.

(54) Szepes, L.; Korányi, T.; Náray-Szabó, G.; Modelli, A.; Distefano, G. *J. Organomet. Chem.* **1981**, *217*, 35.

(not reported) of the germanium dimer (**12**) displays a single broad resonance (~ 1.7 eV, fwhm), centered at 2.6 eV. The spectrum recorded in the "low-rejection" mode, where the signal is correlated to the back-scattering cross section,³⁷ does not supply clear evidence for two overlapped contributions but seems to be consistent with a weak signal (at about 3.7 eV) superimposed on the high-energy side of the first resonance located at 2.5 eV (see Figures 5 and 6). This tentative deconvolution is in line with the finding that also in the dimers of silicon and tin the lowest σ^*_{M-C} resonance is shifted 0.3–0.4 eV to higher energy with respect to the corresponding tetramethyl derivatives. In any case, it is not clear why in the germanium dimer this resonance has a drastically smaller cross section than in the lighter and heavier analogues. A second peculiarity in the germanium dimer is that the LUMO does not fit the trend of decreasing energy observed on going from the silicon to the tin derivative, its ground anion state lying at about 0.2 eV higher energy than in hexamethyldisilane (**2**). In contrast, a sizable electron affinity increase was observed¹¹ in the corresponding group 16 dimers on going from the sulfur to the selenium derivative. Even accounting for the anomalies found in the ET spectrum of hexamethyldigermane (**12**), it can be noted that the energy trends of both the second empty and second filled orbitals in the dimers on going down the group closely parallel those displayed by the LUMOs and HOMOs, respectively, in the monomers. A significantly different nature of the first empty and filled orbitals is further confirmed by the different trend and smaller energy variation along the series. In line with the assignment of the HOMO to the σ orbital mainly responsible for the heteroatom–heteroatom bond, its energy trend parallels the trend in heteroatom–heteroatom bond strengths.⁴³ When the ET apparatus is operated in the "low-rejection" mode in hexamethyldistannane (**13**), two additional resonances are observed at 4.8 and 5.7 eV. Their energy separation is very close to that between the first two occupied orbitals⁵¹ (see Figure 6), so that these two features could be tentatively associated with core excited resonances⁵⁵ in which capture of the extra electron in the LUMO is accompanied by simultaneous electron excitation from the HOMO or from the second occupied orbital, respectively.

Conclusions

Electron transmission spectroscopy demonstrates that the presence of a group 14 heteroatom–heteroatom bond in saturated hydrocarbons causes a sizable electron affinity increase. In a Koopmans' theorem sense, the LUMO, with mainly heteroatom character, is well separated in energy from the higher-lying $\sigma^*_{C-heteroatom}$ empty orbitals. The empty orbital structure reflects the filled counterpart, not only in the dimers but also in the analyzed silicon oligomers. The main difference appears to be a larger energy splitting in the vacant σ^*_{Si-Si} orbitals than in the filled σ_{Si-Si} orbitals, suggesting a large delocalization of the extra electron in the lowest anion states along the Si skeleton. These findings unveil why polysilanes absorb in the UV region at sizably lower energy than the corresponding alkanes, their behavior resembling more that of alkenes. *Ab initio* 3-21G* calculations predict the LUMOs in short linear oligosilanes to be π -shaped orbitals bonding among the silicon atoms, whereas semiempirical calculations describe the nature of the LUMOs in a more classical fashion, that is, with antibonding character among the silicon atoms. Although the ordering of the empty orbital energies calculated in the neutral states is not expected to follow necessarily the ordering of the corresponding anion states, it has been shown⁵⁶ that in most cases, for series of related molecules, a qualitatively correct correlation exists between the LUMO eigenvalues (calculated without the inclusion of diffuse functions) and the corresponding AE values measured in ETS. For the present series of linear oligosilanes (including the monomer) a good linear correlation is found using either the *ab initio* or the MNDO LUMO energies. However, when in addition to the LUMO the higher-lying empty orbitals are considered, the semiempirical results do provide a better match with the experimental AE trends.

Acknowledgment. The authors thank the Italian Ministero dell'Università e della Ricerca Scientifica e Tecnologica and the CNR "Progetto Finalizzato Materiali Speciali per Tecnologie Avanzate" for financial support of this research.

OM950613Y

(55) Sanche, L.; Schulz, G. J. *Phys. Rev.* **1972**, *A6*, 69.

(56) Heinrich, N.; Koch, W.; Franking, G. *Chem. Phys. Lett.* **1986**, *124*, 20.